

Combination of Ferromagnetic and Antiferromagnetic Features in Heisenberg Ferrimagnets

Shoji Yamamoto

*Department of Physics, Faculty of Science, Okayama University,
Tsushima, Okayama 700-8530, Japan*

Takahiro Fukui

*Institut für Theoretische Physik, Universität zu Köln,
Zùlpicher Strasse 77, 50937 Köln, Germany*

Klaus Maisinger and Ulrich Schollwöck

*Sektion Physik, Ludwig-Maximilians-Universität München,
Theresienstrasse 37, 80333 Munich, Germany*

(Received 19 June 1998)

We investigate the thermodynamic properties of Heisenberg ferrimagnetic mixed-spin chains both numerically and analytically with particular emphasis on the combination of ferromagnetic and antiferromagnetic features. Employing a new density-matrix renormalization-group technique as well as a quantum Monte Carlo method, we reveal the overall thermal behavior: At very low temperatures, the specific heat and the magnetic susceptibility times temperature behave like $T^{1/2}$ and T^{-1} , respectively, whereas at intermediate temperatures, they exhibit a Schottky-like peak and a minimum, respectively. Developing the modified spin-wave theory, we complement the numerical findings and give a precise estimate of the low-temperature behavior.

I. INTRODUCTION

Low-dimensional quantum magnets with two kinds of antiferromagnetically exchange-coupled centers have been attracting much current interest. Several authors [1–4] constructed integrable Hamiltonians and extracted suggestive critical phenomena from them. Alternating-spin antiferromagnets with singlet ground states stimulate us to study again the nontrivial gap problem [5]. Employing the nonlinear- σ -model technique, various mixed-spin systems such as linear chains [6,7] and ladders [8] have systematically been studied with particular emphasis on the competition between massive and massless phases.

In this context a remarkable attention has been directed to ferrimagnetic mixed-spin chains [9–18], which are the subject in the present article. Since we may expect gapless excitations from magnetic ground states, it is less interesting there whether the system is massless or massive. Using a field-theoretical argument, Alcaraz and Malvezzi [9] predicted that mixed-spin isotropic Heisenberg ferrimagnets should exhibit quadratic dispersion relations. Their prediction was numerically verified and the quadratic dispersion was explicitly visualized [14]. Thus quantum ferrimagnets are expected to behave like ferromagnets at low temperatures. On the other hand, conventional spin-wave calculations [10,12] and a perturbation approach [14] from the decoupled-dimer limit suggest that quantum ferrimagnets should exhibit nontrivial gapped excitations as well, which have the effect of enhancing the ground-state magnetization and are there-

fore of antiferromagnetic nature. A quantum Monte Carlo (QMC) technique and an exact-diagonalization method [14] actually observed the two distinct low-lying excitations and showed that the mixed nature remains unchanged as long as the model is isotropic.

Motivated by the revealed low-energy structure, two of the present authors [17] have investigated the thermodynamic properties of Heisenberg ferrimagnetic spin chains focusing on the idea of coexisting ferromagnetic and antiferromagnetic aspects. On the one hand, a QMC method was employed to find the overall thermal behavior. On the other hand, a modified spin-wave (MSW) theory was introduced to clarify how the two distinct excitations contribute to the thermodynamics. The present article is a developed richer version of the preceding work. In order to inquire further into the low-temperature behavior, we here employ additional numerical tools. A quantum transfer-matrix (QTM) method allows us to observe how the ferromagnetic character grows with the increase of the system size. A brand-new density-matrix renormalization-group (DMRG) technique helps us to go down into the low-temperature region that was never attained before. Furthermore, taking account of certain interactions between spin waves, we refine the MSW theory so as to bring a more accurate description of the thermal quantities at low temperatures. Although it is rather hard, even with interacting spin waves, to obtain a quantitative description of the overall thermal behavior, a grand-canonical approach to ferrimagnets in terms of spin waves is suggestive enough and interesting in itself. We fully argue how we should *modify* the conventional

spin-wave theory in an attempt to construct the thermodynamics of quantum ferrimagnets.

We consider two kinds of spins S and s alternating on a ring with antiferromagnetic exchange coupling between nearest neighbors, as described by the Hamiltonian

$$\mathcal{H} = J \sum_{j=1}^N (\mathbf{S}_j \cdot \mathbf{s}_j + \delta \mathbf{s}_j \cdot \mathbf{S}_{j+1}) - g \mu_B H \sum_{j=1}^N (S_j^z + s_j^z), \quad (1)$$

where N denotes the number of unit cells, δ represents a bond alternation, μ_B is the Bohr magneton, and we have set the g factors of both spins S and s equal to g . We assume that $S > s$, which remains general enough to describe alternating-spin ferrimagnets. The Lieb-Mattis theorem [19] shows that the Hamiltonian (1), unless a field applied, has $[2(S-s)N+1]$ -fold degenerate ground states. The ferromagnetic and the antiferromagnetic excitations, which lie in the subspaces of $M < (S-s)N$ and $M > (S-s)N$, respectively, indeed show a quadratic dispersion and a gapped spectrum [14], where $M = \sum_{j=1}^N (S_j^z + s_j^z)$ is the total magnetization. The antiferromagnetic gap, namely, the gap between the ground state and the lowest excitation to $M = (S-s)N+1$, was estimated to be $1.75914(1)J$ in the thermodynamic limit. The correlation length of the system is so small that it is barely of the length of the unit cell [10,12] even at the Heisenberg point $\delta = 1$.

II. NUMERICAL STUDY

In this section, using several numerical tools, we calculate the specific heat and the magnetic susceptibility at zero field. The spin-wave [10,12] and the perturbation [14] calculations suggest that the low-temperature properties of the model are qualitatively the same regardless of the values of S and s as long as they differ from each other. Alcaraz and Malvezzi [9] performed finite-size calculations combined with a scaling analysis in the cases of $(S, s) = (1, 1/2)$ and $(S, s) = (3/2, 1/2)$ and indeed concluded that the appearance of quadratic dispersion relations should be expected for arbitrary isotropic mixed-spin chains showing ferrimagnetism instead of antiferromagnetism. Thus we restrict our numerical investigations to the case of $(S, s) = (1, 1/2)$.

A. Procedure

We employ the QMC method based on the Suzuki-Trotter decomposition [20] of the checkerboard type [21]. The partition function $Z = \text{Tr}[e^{-\beta\mathcal{H}}]$ is approximately decomposed as

$$Z \simeq \left[\left(\prod_{i=1,3,\dots} e^{-\beta h_i/n} \prod_{i=2,4,\dots} e^{-\beta h_i/n} \right)^n \right], \quad (2)$$

where n is a Trotter number, $\beta = (k_B T)^{-1}$ with the Boltzmann constant k_B , and

$$\begin{aligned} h_{2j-1} &= J \mathbf{S}_j \cdot \mathbf{s}_j - \frac{1}{2} g \mu_B H (S_j^z + s_j^z), \\ h_{2j} &= J \delta \mathbf{s}_j \cdot \mathbf{S}_{j+1} - \frac{1}{2} g \mu_B H (s_j^z + S_{j+1}^z). \end{aligned} \quad (3)$$

In order to accelerate the thermodynamic calculation and refine its accuracy, we make use of the improved algorithm in Ref. [22]. Calculations are carried out at several values of n and N and they are extrapolated to the limit of $n \rightarrow \infty$ and $N \rightarrow \infty$. Although we have treated chains of $N = 24$, $N = 32$, and $N = 48$, the size dependence of the thermal quantities is so weak that we find no difference beyond the numerical uncertainty even between the calculations at $N = 24$ and $N = 32$ except for very low temperatures. Both the specific heat C and the magnetic susceptibility χ are directly evaluated through formulae [23]

$$C = k_B \beta^2 (\langle Q_2 \rangle + \langle Q_1^2 \rangle - \langle Q_1 \rangle^2), \quad (4)$$

$$\chi = g^2 \mu_B^2 \beta (\langle M_2 \rangle - \langle M_1 \rangle^2), \quad (5)$$

with

$$\begin{aligned} Q_1 &= \sum_{i,m} \left[\frac{\partial \rho_i^{(m)}}{\partial \beta} / \rho_i^{(m)} \right], \\ Q_2 &= \sum_{i,m} \left[\frac{\partial^2 \rho_i^{(m)}}{\partial \beta^2} / \rho_i^{(m)} - \left(\frac{\partial \rho_i^{(m)}}{\partial \beta} / \rho_i^{(m)} \right)^2 \right], \end{aligned} \quad (6)$$

$$\begin{aligned} M_1 &= \frac{1}{2n} \sum_{i,m} \sigma_i^{(m)}, \\ M_2 &= \frac{1}{2n} \sum_m \left(\sum_i \sigma_i^{(m)} \right)^2. \end{aligned} \quad (7)$$

where $\langle A \rangle$ denotes the thermal average of A at a given temperature β^{-1} , $\sigma_i^{(2l-1)}$ and $\sigma_i^{(2l)}$ are Ising spins on the site i at the l th Trotter layer, and the local Boltzmann factors $\rho_{2j-1}^{(2l-1)}$ and $\rho_{2j}^{(2l)}$ are defined in terms of the eigenstates of S_j^z and s_j^z as

$$\rho_i^{(m)} = \langle \sigma_i^{(m)}, \sigma_{i+1}^{(m)} | e^{-\beta h_i/n} | \sigma_i^{(m+1)}, \sigma_{i+1}^{(m+1)} \rangle. \quad (8)$$

As far as we replace the trace by an importance sampling, it is hardly feasible to take grandcanonical averages at very low temperatures. In an attempt to avoid the difficulty, we may integrate out [24,25] the $(1+1)$ -dimensional Ising system but then have to give up either low temperatures or long chains. We can in principle reach an arbitrary low temperature at the expense of the system size and such an attempt is to a certain extent fruitful in the present system whose correlation length is very small. Actually, constructing transfer matrices

in the chain direction, we will later show QTM calculations of the specific heat. Although the QTM calculations themselves are so accurate as to be regarded as exact, numerical differentiations of them may introduce errors. Here we directly calculate the internal energy, rather than the partition function, and numerically differentiate it once. We keep the final results highly accurate by taking raw data at regular intervals of $k_B T/J = 0.01$.

On the other hand, constructing transfer matrices in the Trotter direction, we can partly reveal the thermal behavior of an infinite chain [26]. However, the exponential growth of the matrix size with the increase of n makes our access to low temperatures unfeasible. In order to overcome the difficulty, we introduce the DMRG technique into our investigations. Based on White's original idea [27] developed at $T = 0$, we apply it to the renormalization of transfer matrices [28,29] instead of Hamiltonians. This extension of the DMRG method has recently been applied to the thermodynamics of several low-dimensional magnets [30–32] and indeed brought us plenty of results at very low temperatures.

The core idea of the so-called transfer-matrix DMRG method can be summarized as reaching large n by reducing the size of the transfer matrix with the use of the DMRG algorithm, which is highly successful in obtaining effective low-energy Hamiltonians. We introduce a step-width β_0 and go successively down to lower temperatures $\beta^{-1} = (n\beta_0)^{-1}$ increasing n linearly. The transfer-matrix DMRG calculation is technically different from the original procedure in that we have to handle nonsymmetric density matrices there. In order to avoid the exponential growth of the matrix size, we keep the number of states in the density matrix constant at a predetermined number m throughout the calculation. At each iteration $n \rightarrow n + 1$, we first produce the transfer matrix at the step $n + 1$ by making a matrix product of the transfer matrix at the step n and the local Boltzmann factor (8) with $\beta = n\beta_0$. Next we unite the two transfer matrices at the step $n + 1$ into an augmented matrix of double width in the Trotter direction. We then calculate the left and right eigenvectors of the enlarged matrix with the maximum eigenvalue and construct a density matrix from them. It is the eigenstates corresponding to the m largest eigenvalues of the density matrix that should be retained to give an approximate description of the transfer matrix at the step $n + 1$. The thus-obtained transfer matrix allows us to calculate the free energy at each temperature $\beta^{-1} = (n\beta_0)^{-1}$. We here carry out the direct estimation [29] of the internal energy and the magnetization, which strongly reduces numerical errors in the final results, the specific heat and the magnetic susceptibility.

Obviously the two controllable parameters β_0 and m decide the precision of the transfer-matrix DMRG calculation. The Trotter decomposition is refined as $\beta_0 \rightarrow 0$, whereas the loss of information is reduced as $m \rightarrow \infty$. At high temperatures, we are compelled to work with small Trotter numbers, while few states are discarded. At low temperatures, Trotter numbers are large enough,

whereas many states are lost due to the large number of iterations. Thus, the convergence of the calculation predominantly depends on β_0 at high temperatures, while on m at low temperatures, as was actually observed [32].

As we have conclusive QMC results at high and intermediate temperatures, we are particularly interested in low-temperature findings from the transfer-matrix DMRG calculation. We therefore invest computational resources mainly in augmenting m . Setting $\beta_0 J$ and m to 0.2 and 128, respectively, we have found that at intermediate temperatures the specific heat is somewhat overestimated, whereas at low temperatures the precision almost reaches three digits. Calculations at $m = 80$, $m = 96$ and $m = 128$ fully converge at $T \gtrsim 0.05$ and almost converge at $0.04 \lesssim T \lesssim 0.05$. We were not able to go further down below successfully. This is mainly due to the macroscopically degenerate ground states of ferrimagnets, which imply that a huge number of states must be retained in our access $T \rightarrow 0$.

B. Results

We show in Fig. 1 the temperature dependence of the specific heat of the $(S, s) = (1, 1/2)$ Heisenberg ferrimagnetic spin chain. We find in Fig. 1(a) a good agreement between the QMC and DMRG calculations. At intermediate temperatures, the specific heat exhibits a Schottky-like anomaly typical of antiferromagnets. Let us consider the model at $\delta = 0$ in an attempt to clarify the origin of this characteristic peak. Now the model is decoupled into dimers and the specific heat per unit cell is simply obtained from an isolated dimer, which is a pure two-level system with doubly degenerate ground states and fourfold degenerate excited states separated above by an energy gap $\Delta = 3J/2$. The specific heat is given by

$$\frac{C}{Nk_B} = \frac{r(\beta\Delta)^2 e^{\beta\Delta}}{(e^{\beta\Delta} + r)^2}, \quad (9)$$

where r is the ratio of the degeneracy of the excited states to that of the ground states. Moving away from the decoupled-dimer point, the low-lying states come to exhibit dispersion and macroscopic degeneracy. At the Heisenberg point $\delta = 1$, for N elementary cells, the ground state is $(N + 1)$ -fold degenerate, whereas the lowest antiferromagnetic excited state is $(N + 3)$ -fold degenerate [19]. We note that the isolated dimer may be regarded as the Heisenberg chain of $N = 1$. Now we make an attempt to fit the intermediate-temperature behavior to the curve (9) allowing only a single additional adjustable parameter A :

$$\frac{C}{Nk_B} = \frac{Ar(\beta\Delta)^2 e^{\beta\Delta}}{(e^{\beta\Delta} + r)^2}. \quad (10)$$

Here we replace r and Δ by their values at the Heisenberg point, the degeneracy ratio of the lowest antiferromagnetic excited states to the ground states and the gap between them, respectively:

$$r = \lim_{N \rightarrow \infty} \frac{N+3}{N+1} = 1, \quad \Delta = 1.759J. \quad (11)$$

We obtain a fine fit with $A = 1.7$, which is also shown in Fig. 1(a). We stress that the Schottky-type specific heat (10) not only fits the peak but also well describes the high-temperature decay. Equation (10) combined with the condition (11) gives an asymptotic high-temperature behavior $1.3(\beta J)^2$, which is well consistent with the high-temperature series-expansion result $(\beta J)^2$ [17]. Thus we find that the temperature dependence of the specific heat straightforwardly reflects the antiferromagnetic gap and therefore the model can be treated well as a two-level system unless it is at low enough temperatures $k_B T \ll \Delta \simeq 1.759J$.

On the other hand, the DMRG results fully allow us to guess the $T^{1/2}$ asymptotic behavior characteristic of ferromagnets. This ferromagnetic feature grows as we move toward the Heisenberg point from the decoupled-dimer limit or alternatively as the system size increases. From this point of view, we observe the chain-length dependence of the specific heat in Fig. 1(b). The naive QTM method is most useful in short chains at low temperatures. We find that the antiferromagnetic feature is rather settled even in short chains, whereas the growth of the ferromagnetic feature is relatively slow. The elementary excitations of ferromagnetic nature are predominantly related to spin 1's, while those of antiferromagnetic nature originate from interactions between the two kinds of spins [14]. These excitations may be identified with the local ones within a unit cell in the vicinity of the decoupled-dimer limit, as shown in Fig. 2. Figure 1(b) suggests that the delocalization effect is more essential to the appearance of the ferromagnetic feature. Actually the ferromagnetic excitations constitute a wider band than the antiferromagnetic ones [14].

We show in Fig. 3 the temperature dependence of the magnetic susceptibility times temperature of the $(S, s) = (1, 1/2)$ Heisenberg ferrimagnetic spin chain. We find again that the QMC and DMRG calculations are in excellent agreement. The product χT diverges as T^{-1} at low temperatures, while it approaches $[S(S+1)+s(s+1)]/3 = 11/12$ at high temperatures. The low-temperature divergence is reminiscent of the ferromagnetic susceptibility [35]. We further note that χT shows a minimum while shifting from the quantum ferromagnetic behavior to the classical paramagnetic behavior. Generally χT is a monotonically decreasing function in ferromagnets, while a monotonically increasing function in antiferromagnets [33]. The susceptibilities of gapped antiferromagnets such as Haldane systems vanish exponentially [22,23,34]. Hence the temperature dependence we are observing may be regarded as a ferromagnetic-to-antiferromagnetic crossover. Actually the minimum of χT appears at a temperature around which the specific heat shows the Schottky-like peak.

In sum, a combination of ferromagnetic and antiferromagnetic features in ferrimagnets has been demon-

strated. The DMRG technique has allowed us to have access to very low temperatures. In an attempt at going further down to even lower temperatures, we develop the MSW theory for ferrimagnets [17] in the next section. We not only aim at obtaining the precise description of the low-temperature behavior but are also interested in describing the overall thermal behavior based on the spin-wave picture.

III. MODIFIED SPIN-WAVE APPROACH

For years the conventional spin-wave theory [36–38] was plagued by the difficulty that the zero-field magnetization diverges in low-dimensional magnets. The low-temperature series expansion within the theory only brings us the leading term of the specific heat and nothing correct for the susceptibility. However, imposing a constraint on the magnetization, Takahashi [39,40] succeeded in describing the low-temperature thermodynamics of low-dimensional ferromagnets. His idea was further applied to several quantum antiferromagnets [41–44] and its wide applicability was established. Recently two of the present authors [17] have introduced this modified spin-wave theory into quantum ferrimagnets and demonstrated that it is quite useful in understanding their characteristic features. Here we develop our argument taking into account interactions between spin waves.

A. Dispersion relations

We have observed that the low-temperature thermodynamics well reflects the dispersion relation of the ferromagnetic branch, whereas the intermediate-temperature behavior is well attributed to that of the gapped antiferromagnetic branch. This scenario is indeed supported by the MSW theory [17]. A combination of the ferromagnetic and antiferromagnetic spin waves on which a particular constraint is imposed reproduces the $T^{1/2}$ initial behavior, the Schottky-like peak, and the T^{-2} decay of the specific heat, and the T^{-2} divergence and the T^{-1} decay of the susceptibility (see Fig. 5 and Fig. 6). However, we should be reminded that the conventional spin-wave calculation, based on which we have started our first attempt [17] to construct the thermodynamics, considerably underestimates the antiferromagnetic gap Δ . Consequently, the MSW approach succeeds in reproducing the Schottky anomaly itself, to be sure, but fails in locating it at a correct temperature. In order to obtain a better description, we here refine the original spin-wave theory.

Let us introduce bosonic operators through the Holstein-Primakoff transformation [36]

$$\begin{aligned} S_j^+ &= (2S - a_j^\dagger a_j)^{1/2} a_j, & S_j^z &= S - a_j^\dagger a_j, \\ s_j^+ &= b_j^\dagger (2s - b_j^\dagger b_j)^{1/2}, & s_j^z &= -s + b_j^\dagger b_j, \end{aligned} \quad (12)$$

where we regard S and s as quantities of the same order, that is, $O(S) = O(s)$. The Hamiltonian (1) with $\delta = 1$ and $H = 0$ is expressed in terms of the bosonic operators as

$$\mathcal{H} = E_{\text{class}} + \mathcal{H}_0 + \mathcal{H}_1 + O(S^{-1}), \quad (13)$$

where

$$E_{\text{class}} = -2sSJN, \quad (14)$$

$$\mathcal{H}_0 = J \sum_j \left\{ 2sa_j^\dagger a_j + 2Sb_j^\dagger b_j + \sqrt{sS} \left[(a_j + a_{j+1})b_j + \text{h.c.} \right] \right\}, \quad (15)$$

$$\mathcal{H}_1 = -J \sum_j \left\{ \frac{1}{4} \left[\sqrt{S/s} (a_j + a_{j+1}) b_j^\dagger b_j^2 + \sqrt{s/S} a_j^\dagger a_j^2 (b_j + b_{j-1}) + \text{h.c.} \right] + (a_j^\dagger a_j + a_{j+1}^\dagger a_{j+1}) b_j^\dagger b_n \right\}. \quad (16)$$

The treatment of the quartic interaction (16) is not so canonical as that of the quadratic Hamiltonian (15). A variety of approaches are possible [18]. Here, in an attempt to obtain the dispersion relations beyond the non-interacting spin-wave theory, we first diagonalize \mathcal{H}_0 and next extract corrections from \mathcal{H}_1 .

The Bogoliubov transformation

$$\begin{aligned} \alpha_k &= \cosh\theta_k a_k + \sinh\theta_k b_k^\dagger, \\ \beta_k &= \sinh\theta_k a_k^\dagger + \cosh\theta_k b_k, \end{aligned} \quad (17)$$

combined with

$$\begin{aligned} a_k &= \frac{1}{\sqrt{N}} \sum_j e^{ik(j-1/4)} a_j, \\ b_k &= \frac{1}{\sqrt{N}} \sum_j e^{-ik(j+1/4)} b_j, \end{aligned} \quad (18)$$

and

$$\tanh 2\theta_k = -\frac{2\sqrt{Ss}}{S+s} \cos\left(\frac{k}{2}\right), \quad (19)$$

diagonalizes \mathcal{H}_0 as [10,12]

$$\mathcal{H}_0 = E_0 + J \sum_k \left(\omega_k^- \alpha_k^\dagger \alpha_k + \omega_k^+ \beta_k^\dagger \beta_k \right), \quad (20)$$

where we have taken twice the lattice constant as unity. The first term in (20) is a quantum correction to the ground-state energy of order $O(S^1)$,

$$E_0 = J \sum_k \left[\omega_k - (S+s) \right], \quad (21)$$

with

$$\omega_k = \sqrt{(S-s)^2 + 4Ss \sin^2(k/2)}. \quad (22)$$

The following terms are the ferromagnetic and antiferromagnetic spin-wave modes of order $O(S^1)$, whose dispersion relations are, respectively, given by

$$\omega_k^\mp = \omega_k \mp (S-s). \quad (23)$$

The lower-energy mode shows a quadratic dispersion relation at small k 's, which is consistent with the $T^{1/2}$ initial behavior of the specific heat. On the other hand, the gap between the two branches is exactly J , which considerably contradicts the numerical estimate $1.759J$.

Now we pick up relevant contributions to the dispersions, as well as to the ground-state energy, from \mathcal{H}_1 . Employing the Wick theorem, we rewrite \mathcal{H}_1 as

$$\begin{aligned} \mathcal{H}_1 &= E_1 - J \sum_k \left(\delta\omega_k^- \alpha_k^\dagger \alpha_k + \delta\omega_k^+ \beta_k^\dagger \beta_k \right) \\ &\quad + \mathcal{H}_{\text{irrel}} + \mathcal{H}_{\text{quart}}, \end{aligned} \quad (24)$$

where $\mathcal{H}_{\text{irrel}}$ contains irrelevant terms such as $\alpha_k \beta_k$ and $\mathcal{H}_{\text{quart}}$ contains residual two-body interactions, both of which are neglected in the following. The correction to the ground-state energy, E_1 , and ones to the dispersions, $\delta\omega_k^\pm$, are, respectively, given by

$$E_1 = -2JN \left[\Gamma_1^2 + \Gamma_2^2 + \left(\sqrt{S/s} + \sqrt{s/S} \right) \Gamma_1 \Gamma_2 \right], \quad (25)$$

$$\delta\omega_k^\pm = 2(S+s) \Gamma_1 \frac{\sin^2(k/2)}{\omega_k} + \frac{\Gamma_2}{\sqrt{Ss}} \left[\omega_k \pm (S-s) \right], \quad (26)$$

with

$$\begin{aligned} \Gamma_1 &= \frac{1}{2N} \sum_k (\cosh 2\theta_k - 1), \\ \Gamma_2 &= \frac{1}{2N} \sum_k \cos\left(\frac{k}{2}\right) \sinh 2\theta_k. \end{aligned} \quad (27)$$

In the thermodynamic limit, the key constants Γ_1 and Γ_2 with $(S, s) = (1, 1/2)$ are estimated to be 0.304887 and -0.337779 , respectively. Up to order $O(S^0)$, we end up with the Hamiltonian

$$\mathcal{H} \simeq E_g + J \sum_k \left(\tilde{\omega}_k^- \alpha_k^\dagger \alpha_k + \tilde{\omega}_k^+ \beta_k^\dagger \beta_k \right), \quad (28)$$

where

$$\tilde{\omega}_k^\pm = \omega_k^\pm - \delta\omega_k^\pm, \quad (29)$$

$$E_g = E_{\text{class}} + E_0 + E_1. \quad (30)$$

In Fig. 4 we plot $\tilde{\omega}_k^\pm$ and ω_k^\pm as functions of k at $(S, s) = (1, 1/2)$ with the previous numerical estimates [14] for finite chains. We find that the antiferromagnetic mode is now improved to a great extent. Furthermore the band widths of the two branches, which are exactly the same within the noninteracting spin-wave theory, are now indeed different, due to the interactions. The gap

$\Delta = J$ is replaced by $\Delta = (1 - 2T_2)J \simeq 1.676J$, which is much closer to the exact value $1.759J$. The ground-state energy E_g is also refined: $E_{\text{class}} + E_0 \simeq -1.437J$, while $E_{\text{class}} + E_0 + E_1 \simeq -1.459J$, where the exact value is $-1.454J$.

B. Thermodynamics

Now let us start our MSW theory from the above-obtained improved dispersion relations. At finite temperatures we replace $\alpha_k^\dagger \alpha_k$ and $\beta_k^\dagger \beta_k$ in the spin-wave Hamiltonian by $\tilde{n}_k^\pm \equiv \sum_{n^-, n^+} n^\pm P_k(n^-, n^+)$, where $P_k(n^-, n^+)$ is the probability of n^- ferromagnetic and n^+ antiferromagnetic spin waves appearing in the k -momentum state and satisfies

$$\sum_{n^-, n^+} P_k(n^-, n^+) = 1, \quad (31)$$

for all k 's. Then the free energy at zero field is given by

$$F = E_g + \sum_k (\tilde{n}_k^- \omega_k^- + \tilde{n}_k^+ \omega_k^+) + k_B T \sum_k \sum_{n^-, n^+} P_k(n^-, n^+) \ln P_k(n^-, n^+). \quad (32)$$

We now carry out the minimization of the free energy (32) with respect to $P_k(n^-, n^+)$'s under a particular constraint as well as the trivial constraint (31). The original

$$\frac{C}{Nk_B} = \frac{3}{4} \left(\frac{S-s}{Ss} \right)^{\frac{1}{2}} \frac{\zeta(\frac{3}{2}) \tilde{t}^{-\frac{1}{2}}}{\sqrt{2\pi}} - \frac{1}{Ss} \tilde{t} + \frac{15}{32(S-s)^{\frac{1}{2}}(Ss)^{\frac{3}{2}}} \left[\frac{(S^2 + Ss + s^2)\zeta(\frac{5}{2})}{\sqrt{2\pi}} - \frac{4\zeta(\frac{1}{2})}{\sqrt{2\pi}} \right] \tilde{t}^{\frac{3}{2}} + O(\tilde{t}^2), \quad (37)$$

$$\frac{\chi J}{N(g\mu_B)^2} = \frac{Ss(S-s)^2 \tilde{t}^{-2}}{3} - (Ss)^{\frac{1}{2}}(S-s)^{\frac{3}{2}} \frac{\zeta(\frac{1}{2}) \tilde{t}^{-\frac{3}{2}}}{\sqrt{2\pi}} + (S-s) \left[\frac{\zeta(\frac{1}{2})}{\sqrt{2\pi}} \right]^2 \tilde{t}^{-1} + O(\tilde{t}^{-\frac{1}{2}}), \quad (38)$$

where $\zeta(z)$ is Riemann's zeta function and $\tilde{t} = k_B \tilde{T}/J = k_B T/J\gamma$ with $\gamma = 1 - \Gamma_1(S+s)/Ss - \Gamma_2/Ss$. Surprisingly, the low-temperature series expansions (37) and (38) are exactly the same as the thermodynamic Bethe-ansatz calculations for the spin-1/2 ferromagnet [35] except for γ . Thus we recognize similarities between ferrimagnets and ferromagnets at low temperatures. We note, however, that ferrimagnets of $S = 2s$ should not strictly be identified with spin- s ferromagnets because of the scaling factor γ . With the interactions, the original temperature T is replaced by $\tilde{T}(> T)$ or equivalently the original spins are reduced. Therefore ferrimagnets of $S = 2s$ behaves like spin- $\tilde{s}(< s)$ ferromagnets, at least at low temperatures, which reminds us of the quantum spin reduction [12] in ferrimagnets. The spin-wave theory shows that the staggered magnetization is reduced to $(S+s)N - 2\tau$ with $2\tau = \sum_k [(S+s)/s\omega_k - 1]$.

Unfortunately, in the present model, the constraint introduced above is not useful at all at high temperatures

idea introduced by Takahashi [39,40] was that the zero-field magnetization should be zero. This constraint works quite well especially in ferromagnets, where it serves to control the number of Holstein-Primakoff bosons. Let us apply the same constraint to the present model:

$$\langle S^z + s^z \rangle = (S-s)N - \sum_k \sum_{\sigma=\pm} \sigma \tilde{n}_k^{-\sigma} = 0, \quad (33)$$

where $S^z = \sum_j S_j^z$ and $s^z = \sum_j s_j^z$. Equation (33) claims that the thermal fluctuation $\sum_k \sum_{\sigma} \sigma \tilde{n}_k^{-\sigma}$ should be constrained to take the *classical* magnetization $(S-s)N$. The free energy and the magnetic susceptibility at thermal equilibrium are then given by

$$F = E_g + \mu(S-s)N - k_B T \sum_k \sum_{\sigma=\pm} \ln(1 + \tilde{n}_k^\sigma), \quad (34)$$

$$\chi = \frac{(g\mu_B)^2}{3k_B T} \sum_k \sum_{\sigma=\pm} \tilde{n}_k^\sigma (1 + \tilde{n}_k^\sigma), \quad (35)$$

with

$$\tilde{n}_k^\pm = \frac{1}{e^{(\tilde{\omega}_k^\pm \pm \mu)/k_B T} - 1}, \quad (36)$$

where μ is a Lagrange multiplier due to the condition (33). The susceptibility has been obtained by calculating $\chi = (g\mu_B)^2 (\langle M^2 \rangle - \langle M \rangle^2) / 3NT$ [39]. Equations (34) and (35) are expanded in powers of $T^{1/2}$ at low temperatures as

because it allows the number of bosons of each mode to diverge. Actually, under the condition of zero magnetization, the specific heat becomes a monotonically increasing function. Hence we propose an alternative constraint [17]. Let us consider the minimization of the free energy constraining the *staggered magnetization* to be zero:

$$\langle : S^z - s^z : \rangle = (S+s)N - (S+s) \sum_k \sum_{\sigma=\pm} \frac{\tilde{n}_k^\sigma}{\omega_k} = 0, \quad (39)$$

where the normal ordering is taken with respect to both operators α and β . Equation (39) implies, just as Eq. (33) does, that the thermal fluctuation $(S+s) \sum_k \sum_{\sigma} \tilde{n}_k^\sigma / \omega_k$ should take the *classical* value $(S+s)N$, rather than the renormalized value $(S+s)N - 2\tau$. We note that, based on the naive idea of zero staggered magnetization without the normal ordering, we have

$$\langle S^z - s^z \rangle = (S + s)N - 2\tau - (S + s) \sum_k \sum_{\sigma=\pm} \frac{\tilde{n}_k^\sigma}{\omega_k} = 0. \quad (40)$$

Besides such a phenomenological argument, a more stringent reason drives us to adopt Eq. (39): The condition (39) exactly reproduces the low-temperature series expansions (37) and (38), whereas the condition (40) fails to do. The conventional spin-wave theory at least brings the correct leading term of the specific heat, which is obviously reproduced by the MSW theory with the constraint of zero magnetization. The low-temperature behavior must be inherent in the dispersion relation and should not be influenced by supplementary constraints. Now the set of self-consistent equations (34) and (35) is replaced by

$$F = E_g + \mu(S + s)N - k_B T \sum_k \sum_{\sigma=\pm} \ln(1 + \tilde{n}_k^\sigma), \quad (41)$$

$$\chi = \frac{(g\mu_B)^2}{3k_B T} \sum_k \sum_{\sigma=\pm} \tilde{n}_k^\sigma (1 + \tilde{n}_k^\sigma), \quad (42)$$

with

$$\tilde{n}_k^\pm = \frac{1}{e^{[J\tilde{\omega}_k^\pm - \mu(S+s)/\omega_k]/k_B T} - 1}, \quad (43)$$

where μ is a Lagrange multiplier due to the condition (39).

In the case of $(S, s) = (1, 1/2)$, we have numerically obtained (41) and (42) in the thermodynamic limit and visualize them in Fig. 5 and Fig. 6, where the solid curves represent the calculations starting from the improved dispersion relations $\tilde{\omega}_k^\pm$, while the dashed curves the calculations with ω_k^\pm [17] instead of $\tilde{\omega}_k^\pm$. Though the present calculation including the $O(S^0)$ interactions underestimates the height of the Schottky-like peak, the interactions indeed correct the location of the peak, which emphasizes that the gapped antiferromagnetic spin-wave mode predominantly contributes to this peak. We would like to attribute the discrepancy unsolved to the constraint rather than to the dispersion relations. Even though we adopt the two constraints (33) and (39) simultaneously, the results do not change essentially. This is not so surprising because the two constraints play almost the same role at low temperatures, as the low-temperature series expansions imply, whereas only the constraint (39) is relevant at high temperatures. The precise description of the overall temperature dependence might be obtained with a temperature-dependent constraint, which is not so interesting.

We obtain the best results from the MSW theory at low temperatures. Figure 6(b) fully convinces us of the validity of the present MSW calculation. Figure 5(b) clearly reveals the low-temperature behavior which no numerical tool has succeeded in observing. Takahashi compared his MSW findings [40] for ferromagnets with the spin-1/2 thermodynamic Bethe-ansatz calculations [35] and

found that the MSW theory correctly describes the leading two terms of the specific heat and the leading three terms of the susceptibility in its low-temperature series expansions. We also find that the low-temperature series expansions (37) and (38) coincide with ones of the spin-1/2 ferromagnet to the same extent except for the scaling factor γ . That may be why the MSW and numerical findings for the susceptibility join at higher temperatures than those for the specific heat.

IV. SUMMARY

Developing an analytic argument as well as employing various numerical tools, we have investigated the thermodynamic properties of Heisenberg ferrimagnetic spin chains. Both ferromagnetic and antiferromagnetic aspects lie in the model; they are most clearly exhibited at low and intermediate temperatures, respectively. One might say that mixed-spin chains possess mixed features. We have shown that the MSW theory starting from the improved dispersion relations precisely describes the low-temperature behavior of the model. We appeal to experimentalists to carry out specific heat and susceptibility measurements of mixed-spin materials especially at low temperatures. On the other hand, the Schottky-like peak of the specific heat and the minimum of the susceptibility-temperature product clearly reflecting the antiferromagnetic gap imply that the antiferromagnetic excitations are not smeared out in the ferromagnetic spectra but stand out clearly. Hence neutron-scattering measurements are also encouraged.

ACKNOWLEDGMENTS

The authors would like to thank H.-J. Mikeska, S. Brehmer, and S. K. Pati for their useful comments and fruitful discussions. This work was supported by the Japanese Ministry of Education, Science, and Culture through the Grant-in-Aid No. 09740286 and by a Grant-in-Aid from the Okayama Foundation for Science and Technology. T.F. is supported by JSPS Postdoctoral Fellowship for Research Abroad. Part of the numerical computation was done using the facility of the Supercomputer Center, Institute for Solid State Physics, University of Tokyo.

-
- [1] H. J. de Vega and F. Woynarovich, *J. Phys. A* **25**, 4499 (1992); H. J. de Vega, L. Mezincescu, and R. I. Nepomechie, *Phys. Rev. B* **49**, 13223 (1994).

- [2] S. R. Aladim and M. J. Martins, J. Phys. A **26**, L529 (1993); M. J. Martins, *ibid.* **26**, 7301 (1993).
- [3] M. Fujii, S. Fujimoto, and N. Kawakami, J. Phys. Soc. Jpn. **65**, 2381 (1996).
- [4] B.-D. Dörfel and S. Meißner, J. Phys. A **30**, 1831 (1997).
- [5] F. D. M. Haldane, Phys. Lett. **93A**, 464 (1983); Phys. Rev. Lett. **50**, 1153 (1983).
- [6] T. Fukui and N. Kawakami, Phys. Rev. B **55**, 14709 (1997); *ibid.* **56**, 8799 (1997).
- [7] K. Takano, preprint (cond-mat/9804055).
- [8] T. Fukui and N. Kawakami, Phys. Rev. B **57**, 398 (1998); A. Koga, S. Kumada, N. Kawakami, and T. Fukui, J. Phys. Soc. Jpn. **67**, 622 (1998).
- [9] F. C. Alcaraz and A. L. Malvezzi, J. Phys. A **30**, 767 (1997).
- [10] S. K. Pati, S. Ramasesha, and D. Sen, Phys. Rev. B **55**, 8894 (1997); J. Phys.: Condens. Matter **9**, 8707 (1997).
- [11] A. K. Kolezhuk, H.-J. Mikeska, and S. Yamamoto, Phys. Rev. B **55**, 3336 (1997).
- [12] S. Brehmer, H.-J. Mikeska, and S. Yamamoto, J. Phys.: Condens. Matter **9**, 3921 (1997).
- [13] H. Niggemann, G. Uimin, and J. Zittartz, J. Phys.: Condens. Matter **9**, 9031 (1997); preprint (cond-mat/9712202).
- [14] S. Yamamoto, Int. J. Mod. Phys. C **8**, 609 (1997); S. Yamamoto, S. Brehmer, and H.-J. Mikeska, Phys. Rev. B **57**, June 1 (1998).
- [15] T. Ono, T. Nishimura, M. Katsumura, T. Morita, and M. Sugimoto, J. Phys. Soc. Jpn. **66**, 2576 (1997).
- [16] T. Kuramoto, J. Phys. Soc. Jpn. **67**, No. 5 (1998).
- [17] S. Yamamoto and T. Fukui, Phys. Rev. B **57**, June 1 (1998).
- [18] N. B. Ivanov, Phys. Rev. B **57**, June 1 (1998); N. B. Ivanov, J. Richter, and U. Schollwöck, preprint (cond-mat/9803150).
- [19] E. Lieb and D. Mattis, J. Math. Phys. **3**, 749 (1962).
- [20] M. Suzuki, Prog. Theor. Phys. **56**, 1454 (1976).
- [21] J. E. Hirsch, R. L. Sugar, D. J. Scalapino, and R. Blankenbecler, Phys. Rev. B **26**, 5033 (1982).
- [22] S. Yamamoto, J. Phys. Soc. Jpn. **64**, 4049 (1995).
- [23] S. Yamamoto, Phys. Rev. B **53**, 3364 (1996).
- [24] H. Betsuyaku, Phys. Rev. Lett. **53**, 629 (1984).
- [25] M. Suzuki, Phys. Rev. B **31**, 2957 (1985).
- [26] H. Betsuyaku, Prog. Theor. Phys. **73**, 319 (1985); T. Yokota and H. Betsuyaku, *ibid.* **75**, 46 (1986); H. Betsuyaku and T. Yokota, *ibid.* **75**, 808 (1986).
- [27] S. R. White, Phys. Rev. Lett. **69**, 2863 (1992); Phys. Rev. B **48**, 10345 (1993).
- [28] T. Nishino, J. Phys. Soc. Jpn. **64**, 3598 (1995).
- [29] R. J. Bursill, T. Xiang, and G. A. Gehring, J. Phys.: Condens. Matter **8**, L583 (1996).
- [30] N. Shibata, J. Phys. Soc. Jpn. **66**, 2221 (1997).
- [31] X. Wang and T. Xiang, Phys. Rev. B **56**, 5061 (1997).
- [32] K. Maisinger and U. Schollwöck, Phys. Rev. Lett., in press (cond-mat/9803122).
- [33] J. C. Bonner and M. E. Fisher, Phys. Rev. **135**, A640 (1964).
- [34] S. Yamamoto and S. Miyashita, Phys. Rev. B **48**, 9528 (1993).
- [35] M. Takahashi and M. Yamada, J. Phys. Soc. Jpn. **54**, 2808 (1985); M. Yamada and M. Takahashi, *ibid.* **55**, 2024 (1986).
- [36] T. Holstein and H. Primakoff, Phys. Rev. **58**, 1098 (1940).
- [37] P. W. Anderson, Phys. Rev. **86**, 694 (1952).
- [38] R. Kubo, Phys. Rev. **87**, 568 (1952).
- [39] M. Takahashi, Prog. Theor. Phys. Suppl. **87**, 233 (1986).
- [40] M. Takahashi, Phys. Rev. Lett. **58**, 168 (1987).
- [41] M. Takahashi, Phys. Rev. B **40**, 2494 (1989).
- [42] J. E. Hirsch and S. Tang, Phys. Rev. B **40**, 4769 (1989); S. Tang, M. E. Lazzouni, and J. E. Hirsch, Phys. Rev. B **40**, 5000 (1989).
- [43] S. M. Rezende, Phys. Rev. B **42**, 2589 (1990).
- [44] K. Hida, J. Phys. Soc. Jpn. **65**, 594 (1996).

FIG. 1. Temperature dependence of the specific heat per unit cell: (a) QMC findings (\circ) and DMRG results (\times) at $N \rightarrow \infty$. The dotted line represents the Schottky-type specific heat (2.9). The numerical uncertainty is smaller than the symbol size. (b) QTM calculations at various values of N , where we show the $N \rightarrow \infty$ curve as well, which is obtained by interconnecting the QMC findings at $k_B T/J \geq 0.4$ and the DMRG results at $k_B T/J \leq 0.4$.

FIG. 2. Schematic representations of the $M = N/2$ ground state of the $N = 1$ isolated dimer composed of spin 1 and spin 1/2 and its ferromagnetic (b) and antiferromagnetic (c) excitations. The arrow (the bullet symbol) denotes a spin 1/2 with its fixed (unfixed) projection value. The solid (broken) segment is a singlet (triplet) pair. The circle represents an operation of constructing a spin 1 by symmetrizing the two spin 1/2's inside.

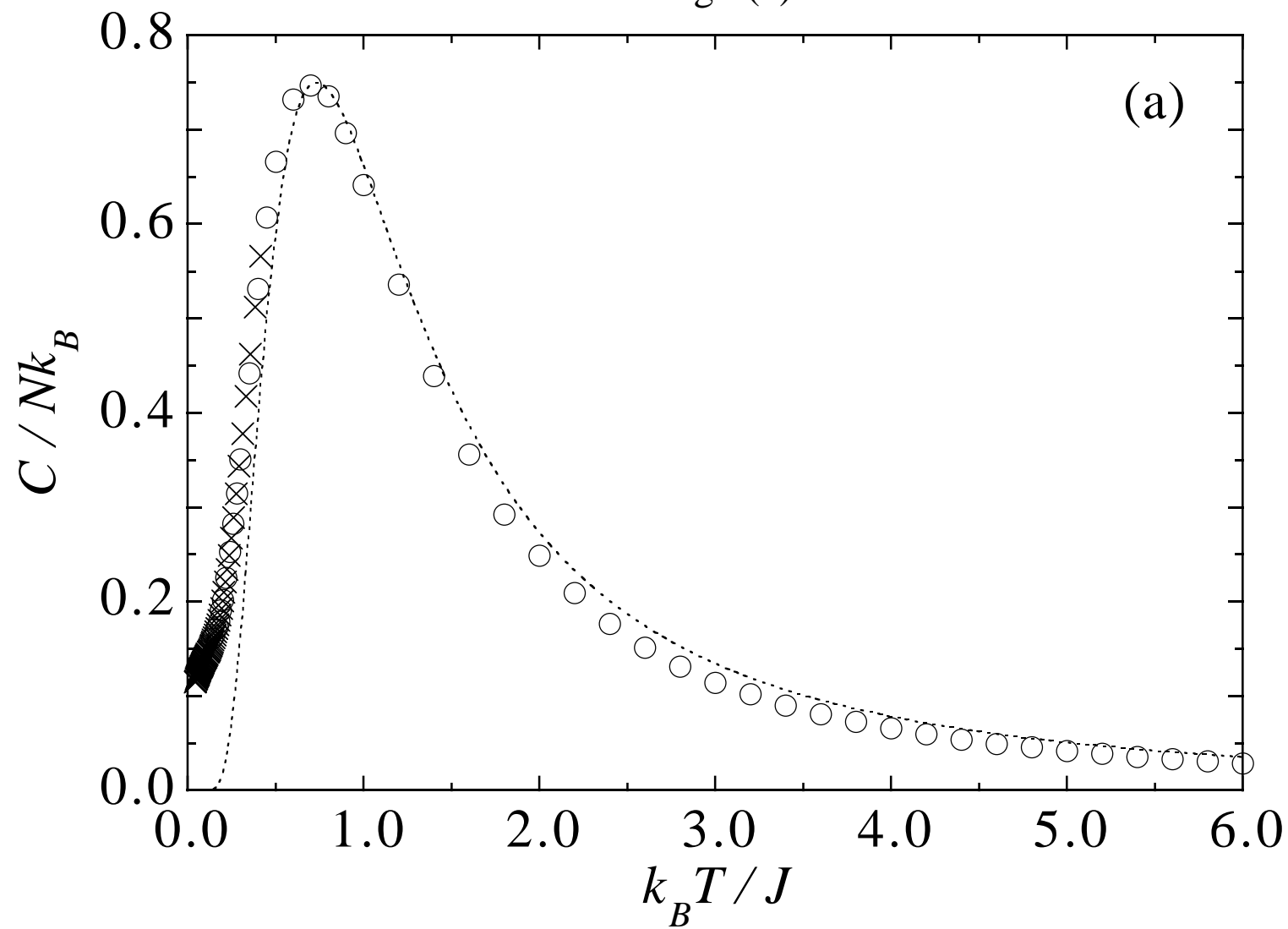
FIG. 3. Temperature dependence of the magnetic susceptibility times temperature per unit cell: QMC findings (\circ) and DMRG results (\times) at $N \rightarrow \infty$. The numerical uncertainty is smaller than the symbol size.

FIG. 4. Dispersion relations of the lowest-energy states in the subspaces of $M = N/2 \mp 1$: The noninteracting spin-wave result (dotted lines) and an improved calculation taking into account interactions between spin waves (solid lines). Previous numerical calculations [14] are also shown for the sake of comparison. Here we plot the excitation energy $E(k)$ taking the ground-state energy and twice the lattice constant as zero and unity, respectively.

FIG. 5. Temperature dependence of the specific heat per unit cell: The MSW calculation with noninteracting spin waves (dotted lines) and that with the improved dispersion relations (solid lines). Numerical findings [QMC (\circ) and DMRG(\times)] are also shown.

FIG. 6. Temperature dependence of the magnetic susceptibility times temperature per unit cell: The MSW calculation with noninteracting spin waves (dotted lines) and that with the improved dispersion relations (solid lines). Numerical findings [QMC (\circ) and DMRG(\times)] are also shown.

Fig.1(a)



(a)

Fig.1(b)

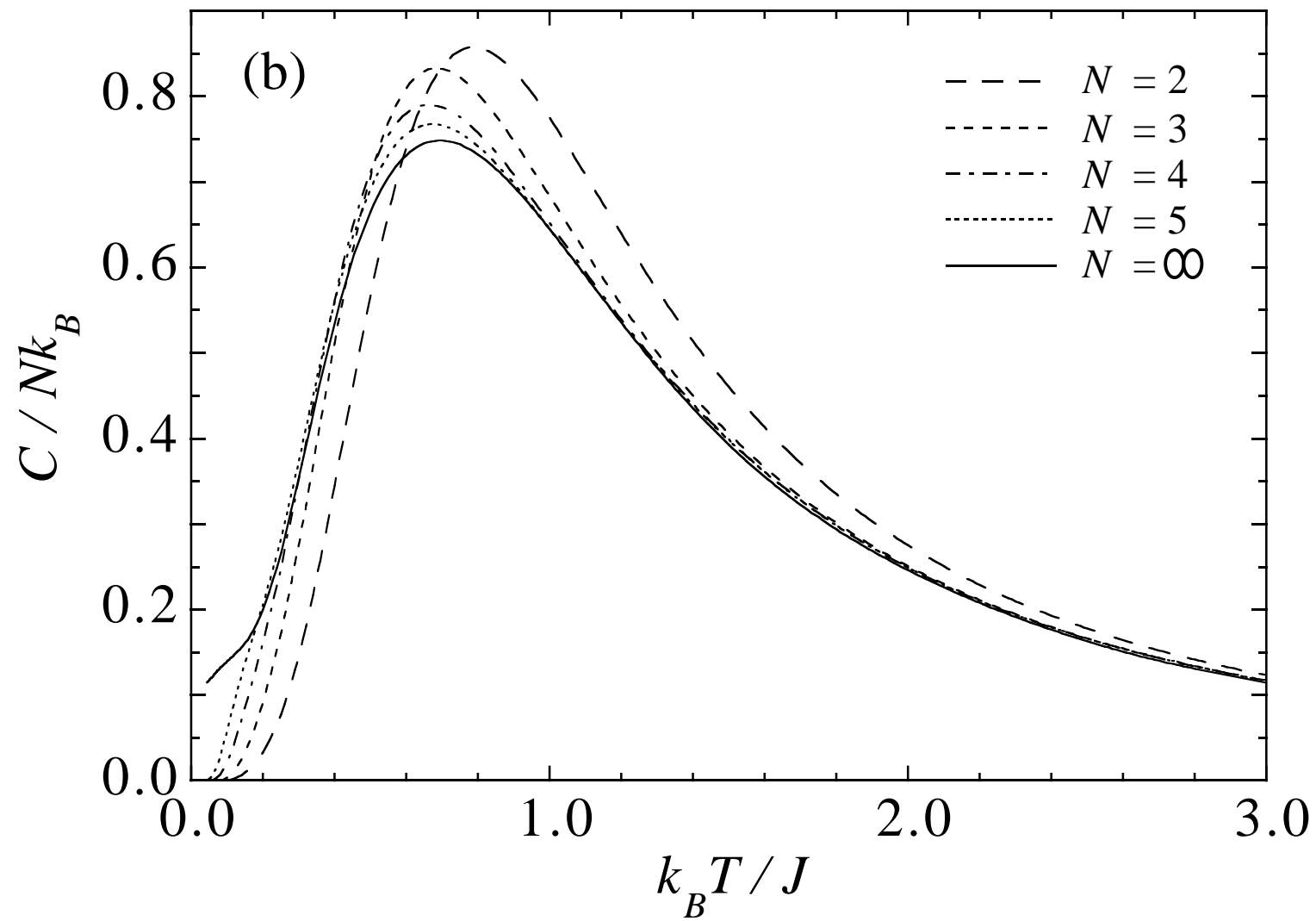
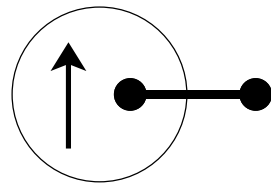
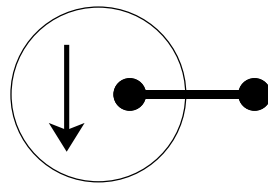


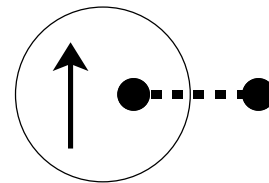
Fig.2



(a)



(b)



(c)

Fig.3

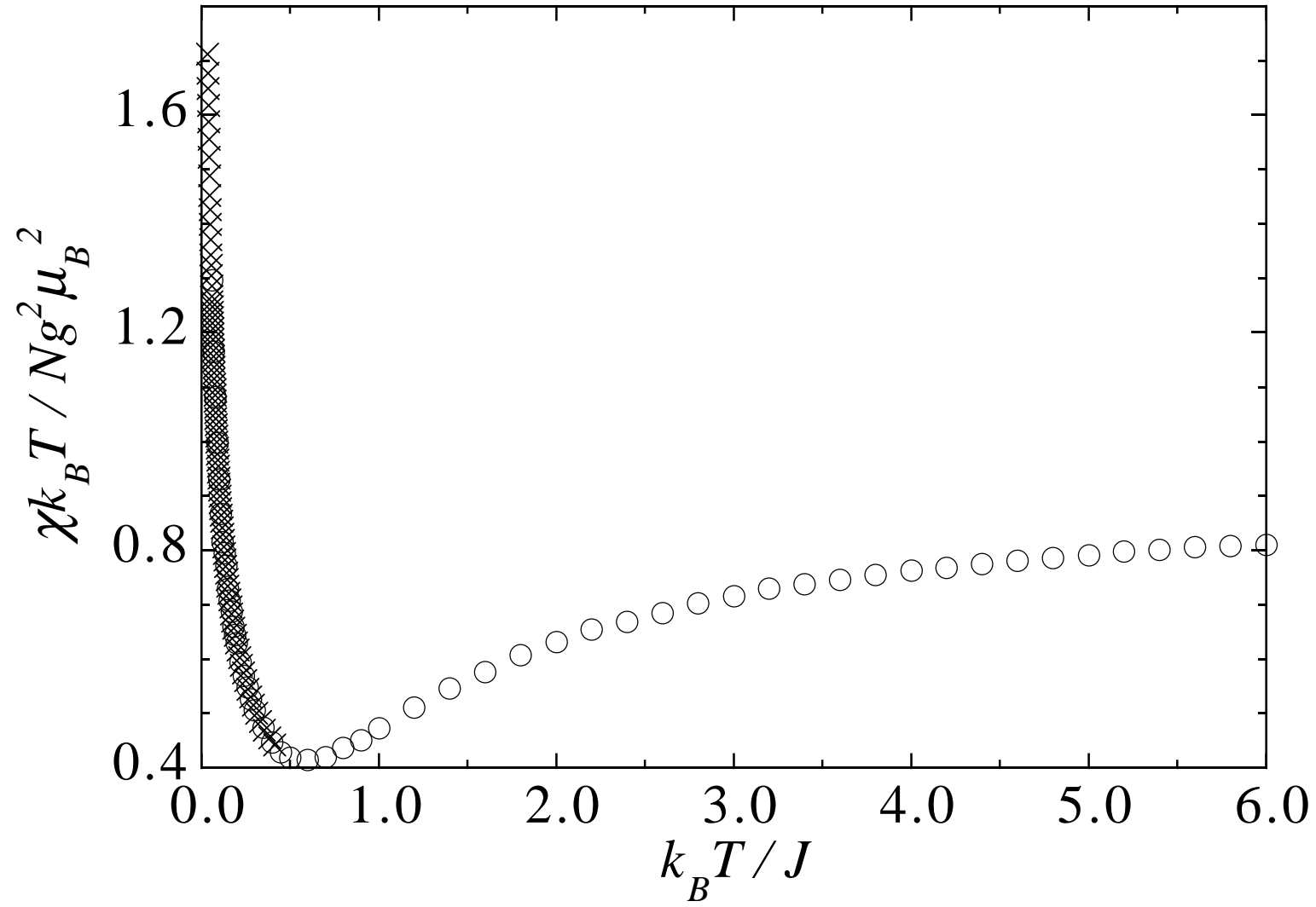


Fig.4

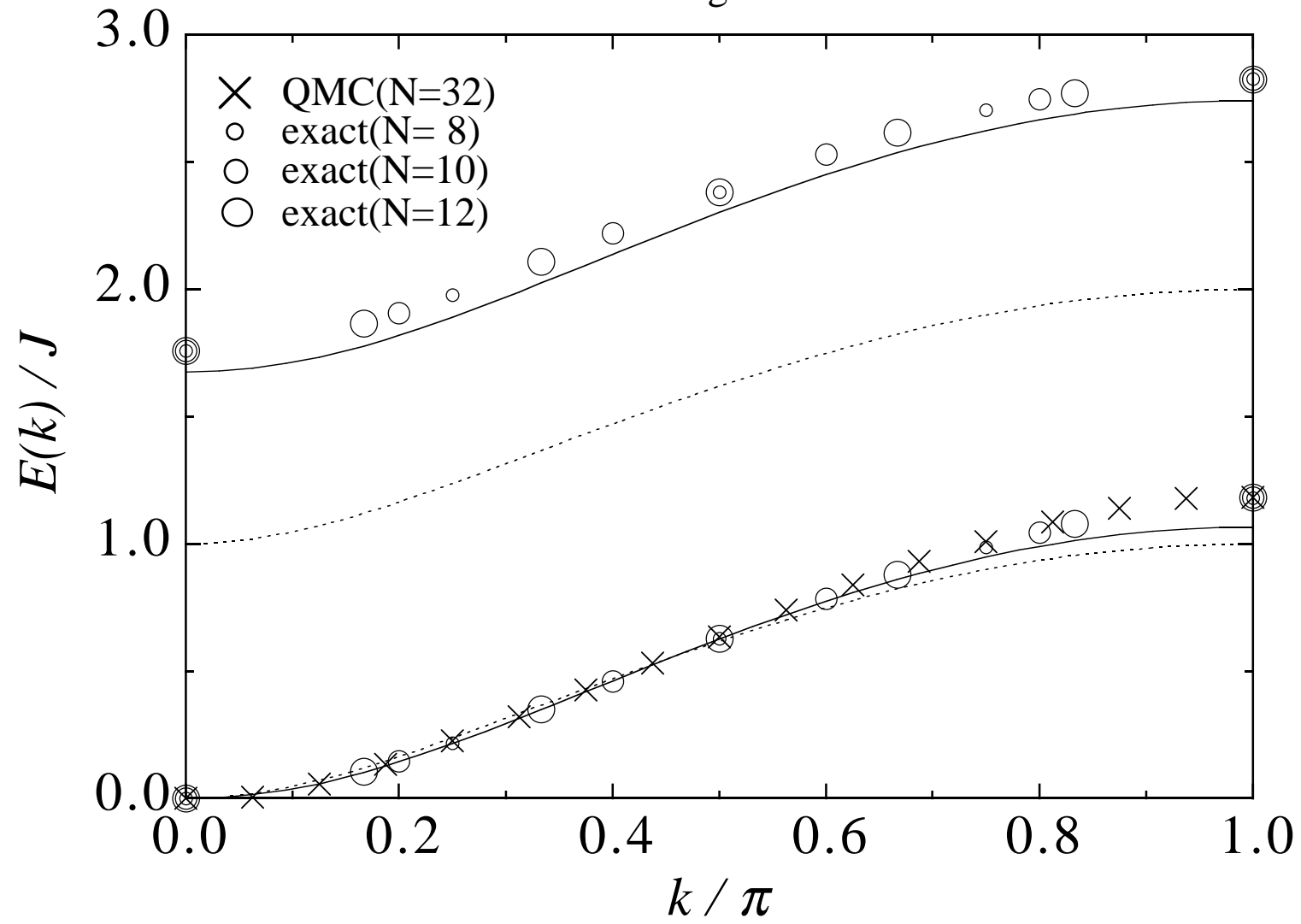


Fig.5(a)

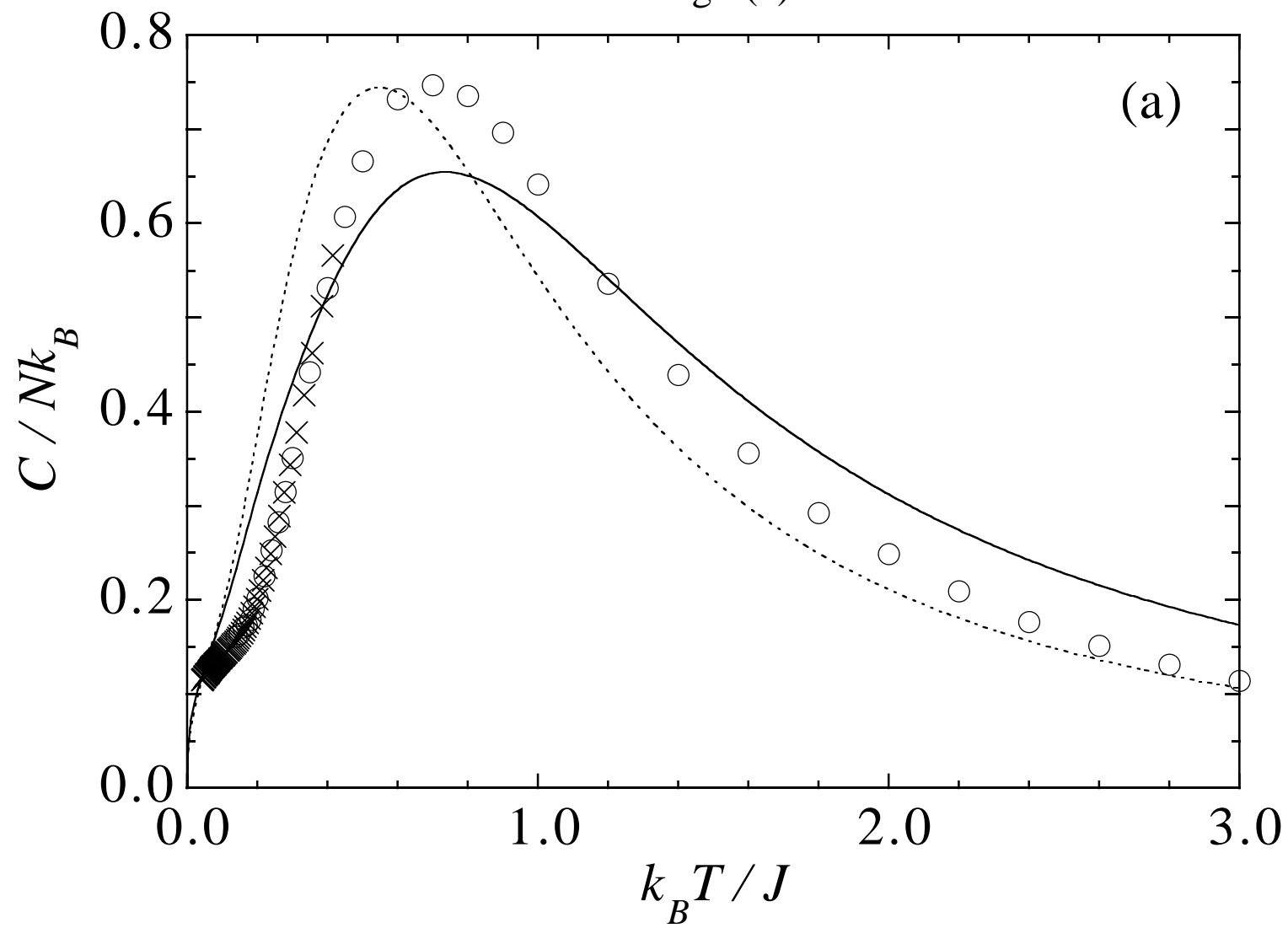


Fig.5(b)

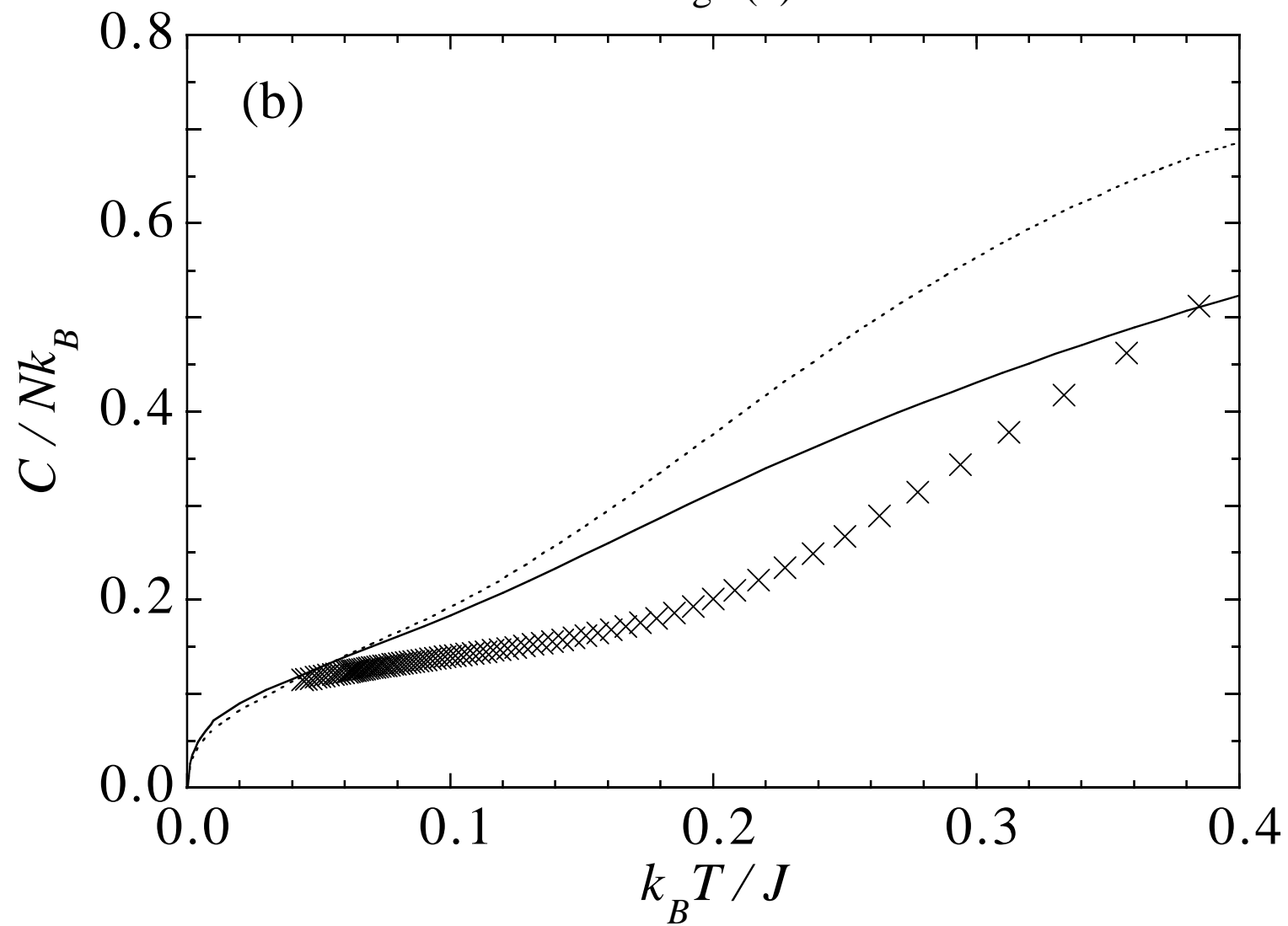


Fig.6(a)

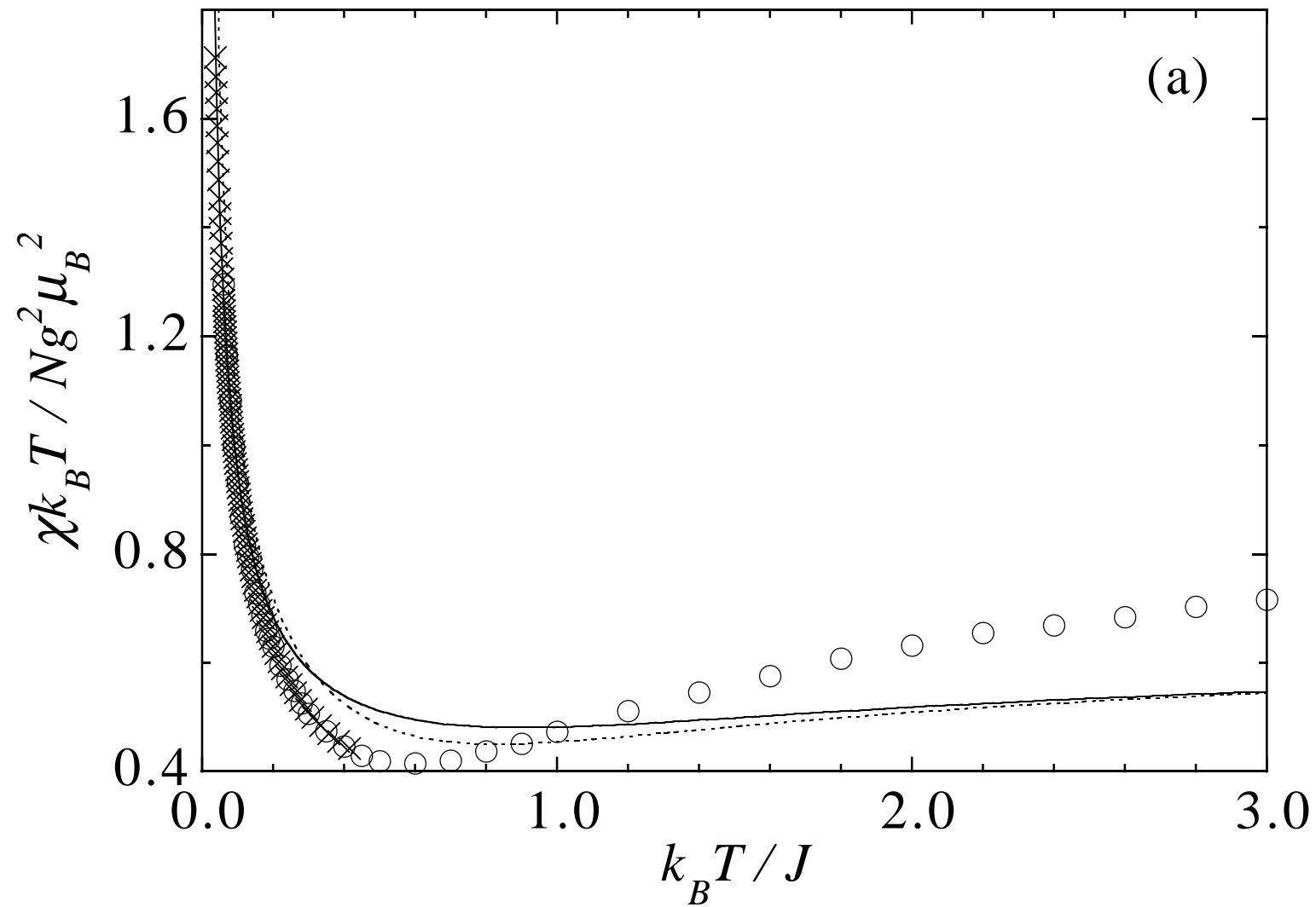


Fig.6(b)

